A Safe Longitudinal Control for Adaptive Cruise Control and Stop-and-Go Scenarios

John-Jairo Martinez and Carlos Canudas-de-Wit

***Abstract*— In this paper, we propose a novel reference model-based control approach for automotive longitudinal control. An important property of this proposed structure concerns the fact that the control design could be meet independent of the model design, permitting the additional control loop only be responsible of the *model-matching* between the actual system and the desired reference dynamics. The reference model is non-linear and provides dynamic solutions consistent with some defined *safety and comfort* constraints. Some model simulations together with some experimental results are presented and discussed.**

***Index Terms*— Automotive, longitudinal control, reference model, adaptive cruise control, stop-and-go.**

I. INTRODUCTION

ADAPTIVE cruise control (ACC), and stop-and-go scenarios are examples of problems related with longitudinal control. The former concerns the inter-distance control in highways where the vehicle velocity mainly remains constant, whereas the latter deals with the vehicle circulating in towns with frequent stops and accelerations. In both situations, goals of safety and comfort most often oppose each other [16].

In most of the reported works, these two categories of problems are treated separately with little regard to the comfort specifications. Indeed, the behavior of the inter-distance dynamics often results from a particular feedback loop, which makes difficult to ensure *a priori* computable bounds on the inter-distance and the vehicle acceleration and its time-derivatives. It is also suited that external factors such as road characteristics, weather conditions, and traffic load (among others), must be considered while defying the safety and the comfort metrics. This last point is naturally reinforced by the new safety programs including vehicles/infrastructure communication [18],[19].

Next we attempts to explain the main ideas about safety and comfort criteria used in automotive longitudinal control. More details and models could be found in [12] and [14].

A. Safe inter-distance policies.

During the last decades the well known "safe inter-distance" has been calculated as a minimal distance to avoid a collision if the preceding vehicle were to act "unpredictably". In fact, the safe inter-distance is calculated from the Newtonian motion equation, permitting to obtain the necessary distance to full stop without collision, some examples are founded in [1], [12], [13], where the safe distance is calculated as

$$d_{safe} = \lambda_1(v_f^2 - v_l^2) + \lambda_2 v_f + \lambda_3, \qquad (1)$$

for some constants λ_1, λ_2, and λ_3. The terms v_f and v_l correspond to the follower and leader velocities, respectively. The first term is related to the relative braking distance between two vehicles; the second term take into account the system reaction time λ_2, the third term λ_3 corresponds to the minimal constant distance to respect.

Part of the attractiveness of this model is that it may be calibrated using common sense assumptions about driver behavior, needing (in the most part) only the maximal braking rates that a driver will wish to use, and predicts other drivers will use, to allow it to fully function. However, this model correspond to a stationary solution of a motion equation, taking a non-exogen input (i.e. it depends of the own speed), and assuming constant and similar decelerations for all the implied vehicles.

Although it produces acceptable results, for example, if one examines the "safety distance" concept, we see that this model is not a totally valid starting point, as in practice, during a urgence maneuver, the vehicles could present so large transitory relative velocity, and then the actual inter-distance tends to decrease abruptly. This is opposed to the reference (1), which indiques that the safe distance should be increased, and by consequence, this safe distance is always violated during a hard stop scenario. Thus, this model could be useful to dictate at what moment the braking maneuver could be started, but it does not supply any braking strategy.

Figure 1 illustrates three different distance policies. One

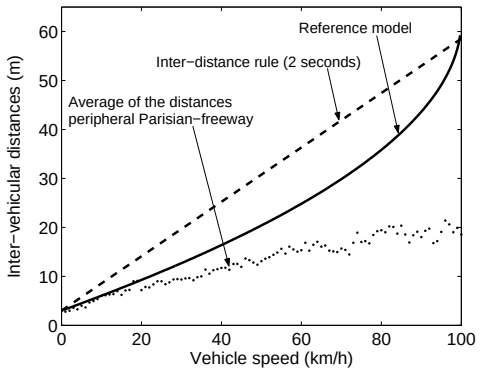

Fig. 1. Comparison of different distance policies: Constant time-headway rule (2 seconds), Average distances in a parisian freeway (source [17]), and the proposed reference distance policy.

Manuscript received January 10, 2005; revised November 7, 2005. This work was supported by the ARCOS French Program.

Authors are with the Laboratoire d'Automatique de Grenoble, CNRS UMR 5528 ENSIEG, INPG, BP.46, St. Martin D'Hères 38440, France.

of these corresponds to the well known *two seconds rule*, that drives are forced to respect. In fact, this rule attempts to respect a distance proportional to the human reaction time (approx. 1.5-2 seconds). Thus, starting from (1), this distance is calculated as

$$d_{safe} = \lambda_2 v_f + \lambda_3. \quad (2)$$

This rule is often called the *Constant Time-headway rule*, where the constant λ_2 stands for the Time-headway.

Many works use this policy as a safe distance, with a little regard in the original safe distance concept. Nevertheless, some variations of this model try to perform other requirements, for example [2] proposes a control strategy where the safety inter-distance is computed as a non-linear function of the speed, (i.e. the Time-headway is a function of the speed), in order to guarantee string stability in the platoon problem.

Returning to the figure 1, we can notice that the current driver behavior (almost in a parisian freeway) is very close to a Constant Time-headway rule. Here, the drivers keep a Time-headway inferior of the usual human reaction time (i.e. less than one second) which is potentially dangerous.

On the other hand, figure 1 also illustrates the proposed reference distance policy, that contrarily to the precedent models, it is obtained from an exogen dynamical motion equation. This fact allows to calculated explicitly the bounds of the model solutions which are obtained through suitable integral curves. Thus, the proposed reference model does not suffer the problems discussed above, that is, we can guarantee safety and comfort requirements in an explicitly way. All this will be discussed in the Section III.

B. Comfort criteria.

Studies on comfort criteria are scarce. However, we can find some works that try to ensure comfort by imitating the human behavior. For example, [3] presents an ACC system for low speed motion, where the desired acceleration was obtained from an estimated model using data of a real driver's behavior. On the other hand, [10] uses human perception theory in order to obtain an acceptable inter-distance reference. The problem here is that reproducing such as behavior may not necessarily lead to safe operation. Therefore, human-based methods may perform over heuristic approaches [19].

In general, passenger comfort in public ground transportation is determined by the changes in motion felt in all directions, as well as by the other environmental effects. Typically, acceleration magnitude is taken as a comfort metric, however in [7] comfort due to the motion changes in a vehicle's longitudinal direction (the "jerk") has been used instead[1]. So, the jerk is important when evaluating the discomfort caused to the passengers in a vehicle. For example, when designing a train and elevators, engineers will typically be required to keep the jerk less than 2 m/s^3 for passenger comfort. Then, an accepted criteria is that bounded longitudinal accelerations and jerks can guarantee a certain degree of comfort in longitudinal control, especially in Stop-and-go scenarios. This aspect will be taken into account during the reference-model design.

[1]the acceleration's time-derivative is the best metric to reflect a human comfort criteria

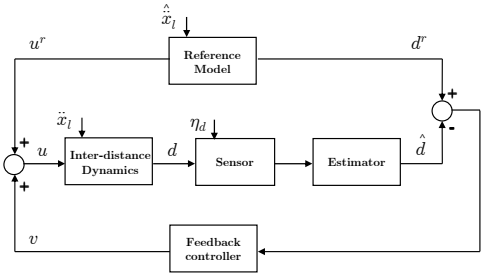

Fig. 2. The inter-distance control scheme.

C. Paper contribution

In this paper, we propose a novel reference model-based control approach for automotive longitudinal control. The proposed structure is intended to allow the controller and the reference model be defined independently. The proposed reference model is nonlinear and provides dynamic solutions which *a priori* verify safety constraints. The model is based on physical laws of compliant contact and has the particularity that its solutions can be described by explicit integral curves. This allows to explicitly characterize the set of initial condition for which the safety constraints can be met. An additional control loop is performed in order to compensates not modelling dynamics and external disturbances. In special, the control is intended to guarantee a good tracking of the desired distance policy (i.e. tracking or model-matching problem).

The remainder of the paper is organized as follows. Section II presents the problem statement. Section III explore the proposed inter-distance reference model. Section IV presents some experimental results. And finally in Section V, we present some conclusions and future directions.

II. PROBLEM STATEMENT

The figure 2 shows the control scheme for which the inter-distance reference model is designed. The longitudinal control problem could be understood as a tracking problem of the inter-distance reference signal $d^r(t)$. With this structure, the controller and the reference model can be defined independently. Thereby, the reference model will include the safety and the comfort constraints, and it could be seen as an exogen system describing a *reference vehicle* dynamics. In that way the controller can be designed to optimally reject other system disturbances specific to the sensors characteristics as well as other disturbance input torques such a side wind, road slopes, and vehicle internal actuator dynamics. We next describe each of the elements of this control scheme.

A. The inter-distance dynamics - The plant

The automotive longitudinal control is generally composed by two loops: an internal or inner control loop which compensates the nonlinear vehicle dynamics (acceleration and brake

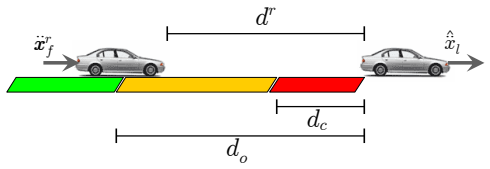

Fig. 3. The inter-distance reference model.

systems), and an outer control loop which is responsible for guaranteeing a good tracking of the desired inter-distance reference. In this work, we assume that the inner control loop has already been designed to compensate the internal vehicle dynamics (acceleration loop), and we are only interested here in the outer control loop, i.e., the inter-distance control loop.

The inter-distance dynamics can be represented as a double integrator driven by the difference between the leader vehicle acceleration $\ddot{x}_l$ and the follower vehicle acceleration $\ddot{x}_f$, i.e.,

$$\ddot{d} = \ddot{x}_l - \ddot{x}_f, \tag{3}$$

where d is the distance between the two vehicles.

B. The reference model

The inter-distance reference model is taken as an exo-system describing a *virtual* vehicle dynamics which is positioned at a distance d^r (the reference distance) from the leader vehicle, as is illustrated in Figure 3. The reference model dynamics is given by

$$\ddot{d}^r = \hat{\ddot{x}}_l - \ddot{x}_f^r, \tag{4}$$

where $\hat{\ddot{x}}_l$ is an estimation of the leader vehicle acceleration and $\ddot{x}_f^r \triangleq u^r(d^r, \dot{d}^r)$ is a nonlinear function of the inter-distance reference d^r and its time-derivative $\dot{d}^r$. This function can be designed to meet safety and comfort requirements, and is related to the safe nominal constant inter-distance, d_o, and the minimal constant inter-distance, d_c, as it will be discussed later.

In order to characterize different safety levels, three zones are defined as follow:

- *Green Zone* : $d^r > d_o$,
  where the inter-distance d is larger than the safe nominal inter-distance d_o (d_o is a *constant* design parameter). This is a safe operation region,

- *Orange Zone* : $d_o \geq d^r > d_c$,
  where $d_o - d_c$ is the necessary inter-distance to avoid collision if a possible hard braking is produced by the leader vehicle.

- *Red Zone* : $d^r \leq d_c$,
  where d_c is a *constant* minimal inter-distance to be respected. This is a collision-free zone.

TABLE I
SAFETY CONSTRAINTS

Collision avoidance	:	$d^r \geq d_c$
Maximum velocity	:	$\dot{x}_f^r \leq V_{max}$
Maximum deceleration	:	$\ddot{x}_f^r \geq -B_{max}$

It is assumed that the velocity and the acceleration of the leader vehicle can be estimated from suitable sensors[2].

On the other hand, the constraints imposed by safety can be set as bounds on the reference vehicle states and its time-derivatives. These constraints are summarized in Table I, where d_c, V_{max}, B_{max} are positive constants. Bounds d_c and V_{max} could be imposed by the driver or by the infrastructure manager, while B_{max} is imposed by the dynamics characteristics of the vehicle. Nevertheless, these bounds may be dependent on the other road external factors as well. In this study, we assume that they are invariant.

C. The reference model-design problem

Introducing $\tilde{d} \triangleq d_0 - d^r$, as being the inter-distance error with respect to the (constant) nominal inter-distance magnitude d_0. The dynamics of this error coordinate will be

$$\ddot{\tilde{d}} = u^r(\tilde{d}, \dot{\tilde{d}}) - \hat{\ddot{x}}_l. \tag{5}$$

The model-design problem is then to find a suitable $u^r = u^r(\tilde{d}, \dot{\tilde{d}})$ such that all the solutions of (5), for a given set of initial conditions (at the moment when orange zone is reached), are consistent with the constraints indicated in Table I. To this aim, we search for suitable nonlinear functions of $u^r(\cdot)$. This is investigated in the Section III.

D. The inter-distance control objective

The control objective is for the inter-distance d, described by the dynamics (3), to track an inter-distance reference signal d^r that satisfies (4). This is illustrated in the Section IV, where it is employed a simple control feedback to solve the model-matching problem for a preliminary experimental benchmark.

Not a lot attention is reserved for the feedback design, and this could be more elaborated in according to each designer. Thus, the proposed control structure and the new reference model design/setting represent the main contribution of this paper.

III. INTER-DISTANCE REFERENCE MODEL.

The inter-distance model-design problem can be studied by making a parallel with the problem of compliant contacts. In particular, nonlinear models resulting from the theory of elasticity and mechanic of the contacts (i.e. Hertz contact model) are a good source of inspiration.

Take for example the following case which considers two different laws for u^r, i.e.

[2]Actually, commercial inter-distance sensors give information about the inter-distance and the relative speed between two cars. Thus, leader speed and/or acceleration should be estimated from these measurements.

$$u^r = \begin{cases} u_1(\cdot) & \tilde{d} < 0 \\ u_2(\tilde{d}, \dot{\tilde{d}}) & \tilde{d} \geq 0 \end{cases} \quad (6)$$

where we assume $\mathcal{C}^1$ continuity between these two structures, i.e. $\frac{\partial u_1}{\partial \tilde{d}}|_{\tilde{d}=0} = \frac{\partial u_2}{\partial \tilde{d}}|_{\tilde{d}=0}$. The particular proposed structure for u^r allows the equation (5) to be re-interpreted as an equation describing the physics of a point mass moving in the free space if $\tilde{d} < 0$, and in contact with a compliant surface if $\tilde{d} \geq 0$.

In this work we assume that in $\tilde{d} < 0$ (i.e. into the green zone), u_1 is dictated by the type of mode selected by the driver (e.g. cruise control or speed regulation). Our interest here is restricted in the "constrained" zone (the orange zone), hence the design of u_2.

Hertz, for example, has proposed a model of the form $u_2 = -k\tilde{d}^n, \forall \tilde{d} \geq 0$, where $n = 1, 2 \cdots$ accounts for contact surface topology. However, the model has the major inconvenient of being non-dissipative, producing a oscillatory effect that may induce a non feasible *negative* vehicle velocity. To cope with this problem, Hunt and Crosseley [8], and then Marhefka and Orin [9] have introduced a non-linear damper/spring model of the general form $u_2 = -c|\tilde{d}|^n\dot{\tilde{d}} - k\tilde{d}^n$, $\forall \tilde{d} \geq 0$. Then, the forces are proportional to the penetration of the object into the surface. One of the advantages of this model is that in connection with (5), it is possible to compute the integral curves associated to the autonomous nonlinear differential equation of the form:

$$\ddot{\tilde{d}} + c|\tilde{d}|^n\dot{\tilde{d}} + k\tilde{d}^n = 0, \qquad \forall n.$$

However, with $k \neq 0$, this equation has a"bouncing" effect; solution of this equation may produce motion with velocity reversal. It is clear that in our framework, we may want that the vehicle velocity behaves monotonically in the forward direction. For this, we can remove the storage-term in the damper/spring model discusses previously and let u_2 be only defined by a dissipation term as (for $n = 1$):

$$u_2 = -c|\tilde{d}|\dot{\tilde{d}}, \quad \forall \tilde{d} \geq 0, \quad (7)$$

which leads to the following equation

$$\ddot{\tilde{d}} = -c|\tilde{d}|\dot{\tilde{d}} - \ddot{\hat{x}}_l. \quad (8)$$

Due to the necessity of eliminating the excess in kinetic energy that the vehicle has once it enters in the orange zone, it is then natural to only use a dissipation term to avoid collisions. Note that the goal of this structure is not to regulate back the reference vehicle to $\tilde{d} = 0$, but to stop the vehicle before it reaches the critical distance d_c, while respecting the imposed comfort constraints as it is illustrated in figure 4.

Consider for simplicity $t = 0$ the time at which the orange zone is reached. Let Ω_0^{orange} be defined as

$$\Omega_0^{orange} = \left\{ \dot{x}_f^r(0), \tilde{d}(0) : \dot{x}_f^r(0) = V_{max}, \tilde{d}(0) = 0 \right\},$$

the set of all admissible initial state values at the crossing point $\tilde{d} = 0$. Now, the problem is to find a value for c and for the constant d_0 (the design parameters of (8)), such that the restrictions in Table I will be satisfied for all possible solutions of (8) starting in Ω_0^{orange}.

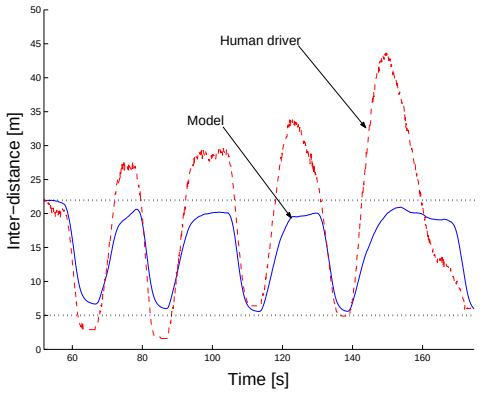

Fig. 4. Inter-distance produced by a human driver vs. that produced by the proposed model. With $d_c = 5m$, $d_0 = 22m$, $B_{max} = 10m/s^2$ and $V_{max} = 15m/s$.

A. Setting the Model

Note that Equation (8) can be solved analytically, i.e.,

$$\dot{\tilde{d}}(t) = -\frac{c}{2}\tilde{d}(t)^2 - \dot{\hat{x}}_l(t) + \beta, \quad (9)$$

with $\beta \triangleq \dot{x}_f^r(0) + \frac{c}{2}\tilde{d}^2(0)$. Note that by definition $\tilde{d}(0) = 0$, then $\beta = \dot{x}_f^r(0)$. Upon substitution of the relation $\dot{x}_f^r(t) = \dot{\tilde{d}}(t) + \dot{\hat{x}}_l(t)$ in (9) one can obtain an explicit relation between the reference vehicle velocity and the "penetration" distance, i.e.

$$\dot{x}_f^r(t) = -\frac{c}{2}\tilde{d}(t)^2 + \beta. \quad (10)$$

From this expression, we can find a c such that for all $\beta = \dot{x}_f^r(0) = V_{max}$, the critical distance d_c is not attained. From:

$$\tilde{d}(t) = \sqrt{\frac{2(\beta - \dot{x}_f^r(t))}{c}}, \quad (11)$$

the maximum penetration distance $\tilde{d}_{max}$ can be computed as $\tilde{d}_{max} = \sqrt{\frac{2\bar{\beta}}{c}}$; ($\bar{\beta} \triangleq \max_{\forall t}\{\beta - \dot{x}_f^r(t)\} = \beta$). Making $\tilde{d}_{max} \leq d_o - d_c$, ($d_o - d_c$ is the orange zone length), we have,

$$\tilde{d}(t) \leq \sqrt{\frac{2\beta}{c}} \leq d_o - d_c, \quad (12)$$

which imposes us a first constraint, $\mathcal{C}_1$, on the possible values of c, i.e.

$$\mathcal{C}_1 : \quad c \geq \frac{2\beta}{(d_o - d_c)^2}. \quad (13)$$

Figure 5 displays the integral curves (10) for different initial reference vehicle velocities. The constant c is computed to ensure that the vehicle inter-distance d^r is larger than d_c for different initial velocities $\dot{x}_f^r(0)$ and $\tilde{d}(0) = 0$.

By taking the time-derivatives on (10), and using (9), we get

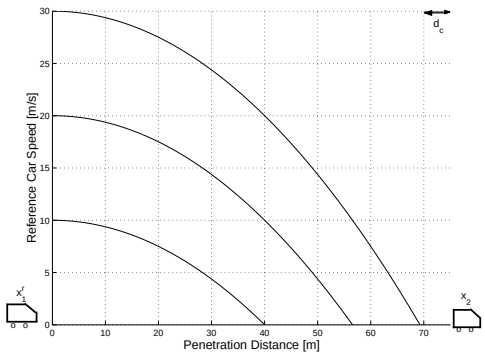

Fig. 5. Speed vs. Penetration Distance for different initial velocities. ($c = 0.0125$, $d_o = 75m$ and $d_c = 5m$).

$$\ddot{x}_f^r = -c|\tilde{d}|[-\frac{c}{2}\tilde{d}^2 + \beta - \dot{x}_l(t)], \tag{14}$$

proceeding in the same way as before, and introducing the deceleration constraint, $\ddot{x}_f^r(t) \geq -B_{max}$ we have:

$$\ddot{x}_f^r(t) \geq -\frac{2}{3}\beta\sqrt{\frac{2c\beta}{3}} \geq -B_{max}. \tag{15}$$

Appendix I presents more details on the derivation of (15).

Figure 6 shows solutions of (8) by different values of c. Notice for example that high values of c yield high values for deceleration and jerk magnitudes, while small values for c are required to get large stoping distances. This relation demonstrates clearly the tradeoff between safety (that require large c), and comfort (that associate small c).

Relation (15) yields an upper bound for c, i.e.

$$\mathcal{C}_2 \quad : \quad c \leq (\frac{27}{8})\frac{B_{max}^2}{\beta^3}. \tag{16}$$

The problem can thus be formulated as finding a value of c , subject to the set of constraints $\mathcal{C}_1$ and $\mathcal{C}_2$. Therefore, a sufficient condition so that c exists is that $\mathcal{C}_1$ and $\mathcal{C}_2$ holds, i.e.

$$\frac{2\beta}{(d_o - d_c)^2} \leq (\frac{27}{8})\frac{B_{max}^2}{\beta^3}, \tag{17}$$

which together with $\beta = V_{max}$, implies that the design parameter d_o should meet the following relation

$$d_o \geq \sqrt{\left(\frac{16}{27}\right)\frac{V_{max}^2}{B_{max}}} + d_c, \tag{18}$$

If d_o is selected according by taking the smaller value compiling with (18), i.e.

$$d_o = \sqrt{\left(\frac{16}{27}\right)\frac{V_{max}^2}{B_{max}}} + d_c, \tag{19}$$

then we can calculate c from $\mathcal{C}_2$, as:

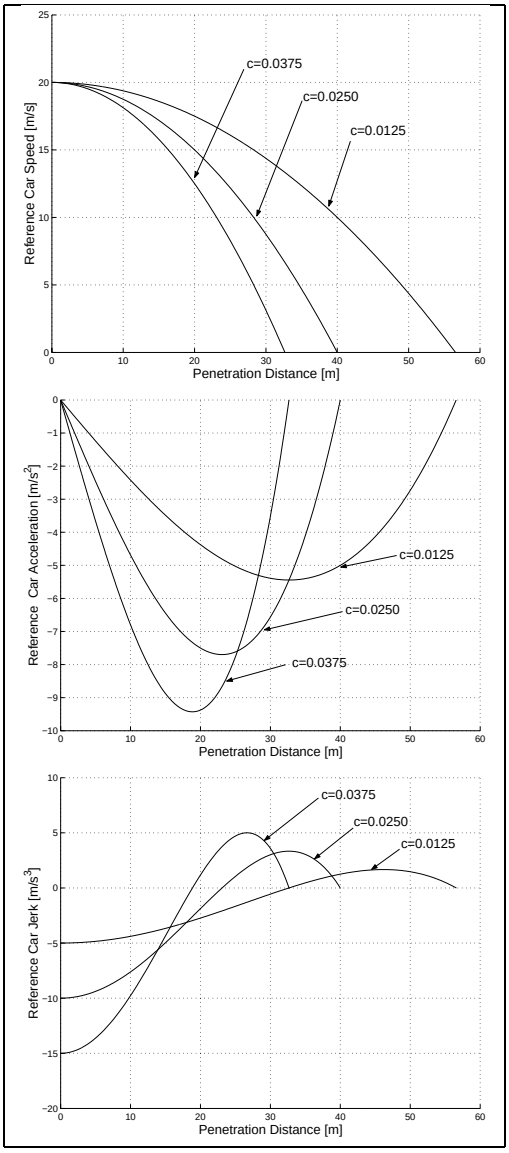

Fig. 6. Speed, Acceleration and Jerk vs. Penetration Distance for the same initial conditions ($\dot{x}_f^r(0) = 20m/s; \tilde{d}(0) = 0m$), and different c values.

$$c = \frac{27B_{max}^2}{8V_{max}^3}. \tag{20}$$

Note that the design parameters could be obtained from (18) and (20) as functions of the imposed bounds d_c, V_{max} and B_{max}. If (18) and (20) hold, the reference inter-distance model provides an inter-distance reference d^r that avoids collision respecting the maximum braking capacity. All this is true for all initial conditions that satisfy $\dot{x}_f^r(0) + \frac{c}{2}\tilde{d}^2(0) = \beta = V_{max}$.

Notice also that the equation (18) gives an important relationship between the maximal vehicle velocity and the safe inter-distance d_o for a given braking capacity B_{max}. In fact, equation (18) corresponds to the braking distance dictated by the model. This braking distance is quite similar to the Newtonian braking distance, equation (1) (i.e. both are quadratic functions of the speed). The figure 7 illustrates this relationship.

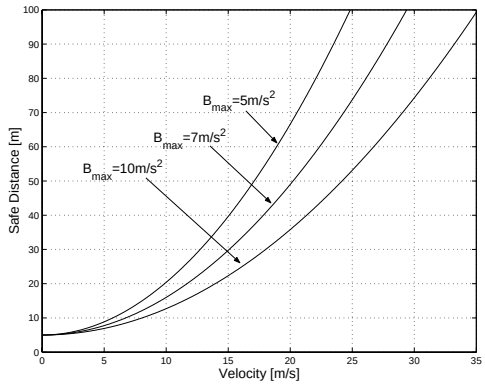

Fig. 7. The distance d_0 as a function of the maximum velocity (See equation (18)), for $d_c = 5m$ and different braking capacities.

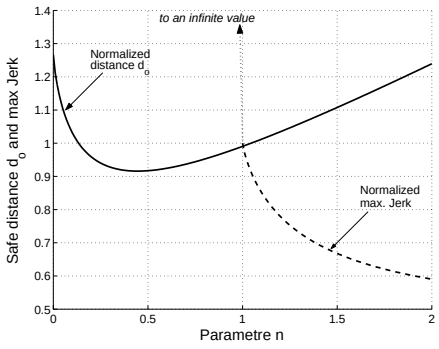

Fig. 8. Safety distance d_o and maximum jerk w.r.t. the parameter n.

B. The comfort behavior

A comfortable braking is here understood as the ability to decelerate with "low" jerk while respecting the safe stopping distance. One of the principal advantages of the proposed reference model, concerns the possibility of evaluate the expected comfort behavior using the solutions of the equation (9). Taking the times-derivatives of (9) in function of $\tilde{d}$, we have the reference acceleration given by

$$\ddot{x}_f^r = -c|\dot{\tilde{d}}| \left[-\frac{c}{2}\tilde{d}^2 + \beta - \hat{\dot{x}}_l(t) \right], \tag{21}$$

and the reference jerk given by

$$\begin{aligned} \dddot{x}_f^r = &- c \left[\dot{\tilde{d}} \left(-c\dot{\tilde{d}} \left\{ -\frac{c}{2}\tilde{d}^2 + \beta - \hat{\dot{x}}_l(t) \right\} - \hat{\ddot{x}}_l(t) \right) \right. \\ &\left. + \left(-\frac{c}{2}\tilde{d}^2 + \beta - \hat{\dot{x}}_l(t) \right)^2 \right]. \end{aligned} \tag{22}$$

Thus, assuming that the estimated leader vehicle acceleration/deceleration is bounded as:

$$-\gamma \leq \hat{\ddot{x}}_l(t) \leq \alpha, \tag{23}$$

where γ and α are positive constants, with $\gamma >> \alpha$, we can re-write (21) and (22) as

$$\ddot{x}_f^r(t) \leq \alpha, \tag{24}$$

$$|\dddot{x}_f^r(t)| \leq \max(c\beta^2, \sqrt{2c\beta}\gamma). \tag{25}$$

These equations (see appendix I and II for derivations), suggest that the maximum positive reference vehicle acceleration and the jerk depend of the chosen design parameter c and the constant β ($\beta = \dot{x}_f^r(0)$), but also depend of the maximum leader vehicle acceleration α and deceleration γ.

Taking, for example, the parameter c as it is calculated in (20) we can, under assumption (23), bound the reference vehicle jerk as:

$$|\dddot{x}_f^r(t)| \leq \max(\frac{27}{8}\frac{B_{max}^2}{V_{max}},\ 2.6\frac{B_{max}}{V_{max}}\gamma). \tag{26}$$

The vehicle safety is then guarantee for all operation conditions, while the vehicle comfort level is adapted to each scenario according to the acceleration/deceleration capabilities of the leader vehicle.

C. Influence of different values of n

We have, until now, analyzed the model with $n = 1$ in (8). Proceeding in the same way, as in Section III-A, and considering different values of the parameter n, we can obtain a more general expression of (18):

$$d_o \geq \left[\frac{n^n (n+1)^{2(n+1)}}{(2n+1)^{2n+1}} \right]^{\frac{1}{n+1}} \frac{V_{max}^2}{B_{max}} + d_c. \tag{27}$$

Similarly, if condition (27) is satisfied, then there exists c such that the maximum braking value B_{max} is respected and the inter-distance is always larger or equal than minimal inter-distance d_c, (for all initial speed smaller or equal to V_{max}), i.e. the parameter c could be calculated as follow:

$$c = \frac{1}{n^n} \left[\frac{2n+1}{n+1} \right]^{2n+1} \frac{B_{max}^{n+1}}{\beta^{2n+1}}. \tag{28}$$

In addition, (27) suggests the existence of a minimum value for d_o as a function of n. Figure 8 illustrates this. Although reducing n gives a smaller safe distance d_o, the comfort may be affected. Figure 8 also shows a numerical plot of the maximum possible jerk values with respect to n, assuming $\max_{\forall t}\{\dot{x}_f^r(0) - \hat{\dot{x}}_l(t)\} = V_{max}$, and $-\gamma \leq \hat{\ddot{x}}_l(t) \leq \alpha$.

$$\begin{aligned} \dddot{x}_f^r = &-cd\tilde{}^n [\tfrac{c^2 \tilde{d}^{2n+1}}{n+1} - cd\tilde{}^n (\dot{x}_f^r(0) - \hat{\dot{x}}_l) - \hat{\ddot{x}}_l] \\ &-cnd\tilde{}^{n-1} [-\tfrac{cd\tilde{}^{n+1}}{n+1} + \dot{x}_f^r(0) - \hat{\dot{x}}_l]^2. \end{aligned} \tag{29}$$

Note that the maximum possible jerk explose to the infinity values for $n < 1$, and it decrease for larger values of n. However the distance d_o (that determines the length of the orange zone), becomes larger for larger n. That means that we can set the model in order to obtain more comfort, *tourist mode* , requiring more distances, or we can set the model for smaller safe distances, *sporting mode*, demanding more jerk.

In the rest of the paper we continuous to use $n = 1$, which concerns a raisonnable value of inter-distance with bounded jerk.

D. Model simulations

1) Case 1: Simulations without noise: To illustrate the behavior of the proposed inter-distance model, we have designed a test profile including cruise control, hard-stop, and stop-and-go scenarios. The simulations have been done considering $V_{max} = 30m/s$, $B_{max} = 10m/s^2$, and $d_c = 5m$. These values are used to compute d_0, and c as shown in previous section. This results in $d_0 = 75m$ and $c = 0.0125$. Initial conditions are $x_1^r(0) = 0m$, $x_2(0) = 85m$, $\dot{x}_1^r(0) = 30m/s$, and $\dot{x}_l(0) = 20m/s$. The dotted lines in the figure 9 shows the curves produced by the simulated leader vehicle.

When the reference vehicle comes near to the leader vehicle, the velocity is adapted with comfortable deceleration and the reference vehicle is positioned to a safe distance. Then, at $t = 25s$ the leader vehicle is stopped with elevate braking value (approximately $10m/s^2$), while the reference vehicle obtains completed stop before critical distance $d_c = 5m$ with a braking smaller than $6m/s^2$. Thereafter, the leader vehicle is accelerated and decelerated (stop-and-go) with usual acceleration values but elevate jerk; however, the reference vehicle is maintained to a safe distance, and a bounded jerk ($< 3m/s^3$).

Figure 9 shown the resulting inter-distance evolution predicted by the virtual vehicle along the complete test-profile. As expected, the red zone is never reached while the acceleration and jerk are keep within the predicted limits.

2) Case 2: Simulations with noise or bias: Here we simulate the reference model driving by a leader vehicle acceleration affected by noise or a bias, i.e.

$$\hat{\ddot{x}}_l = \ddot{x}_l + \eta_l, \tag{30}$$

where η_l could be a zero mean, gaussian noise signal, with variance equal to 0.1 (Figure 10), or a bias equal to $0.1m/s^2$ (Figure 11).

The minimal inter-distance and the maximal braking is always respected as a consequence of assuring the leader dynamics hypothesis dictated in Section III-A, i.e. the estimated leader dynamics (30) is subject to:

$$0 \quad \leq \quad \hat{\dot{x}}_l(t) \quad \leq V_{max}, \quad \forall t. \tag{31}$$

Figure 10 illustrates the response of the reference model when it is driven by an noisy leader acceleration. Note that the reference model always respect the minimal inter-distance with bounded jerk. Note also that the effect of a noisy measurement only is observed in the jerk response that becomes noisy too.

On the other hand, figure 11 illustrates the response of the reference model when it is driven by a leader acceleration affected by a constant bias. Notice that the reference inter-distance response changes a little with respect to the above case. However, the minimal inter-distance is always respected with bounded jerk. During braking, the positive jerk becomes bigger than the above case. Notice too that due to the bias the maximal inter-distance decrease a little. These aspects

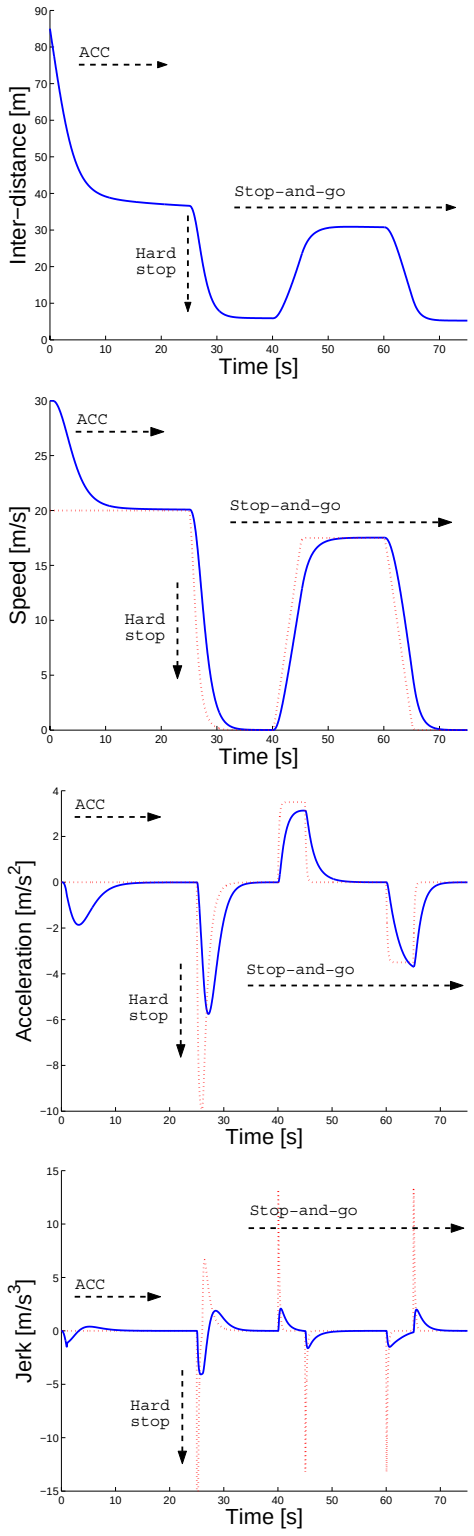

Fig. 9. Inter-distance, velocities, acceleration and jerk for a given leader profile.

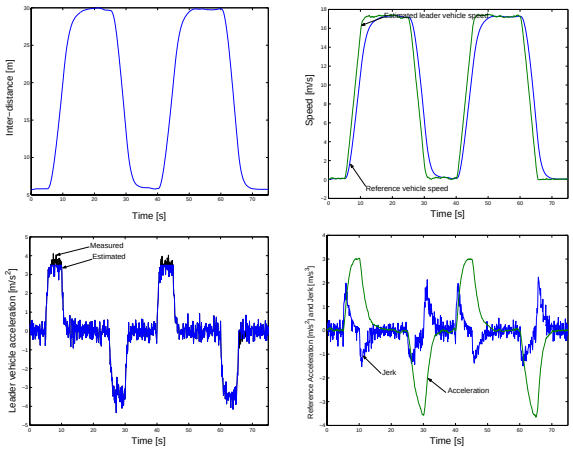

Fig. 10. Behavior of the model affected by *noise* in the leader acceleration measurement.

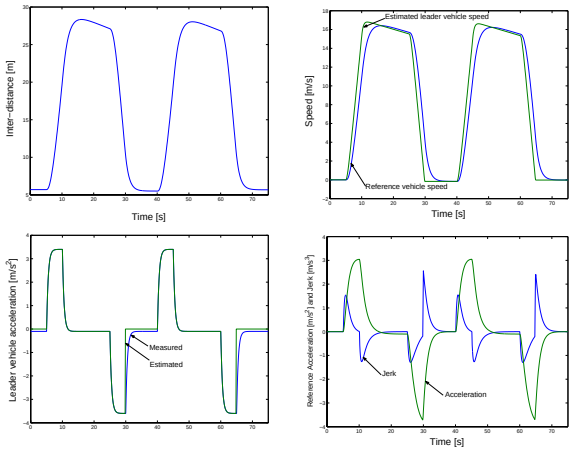

Fig. 11. Behavior of the model affected by a *bias* in the leader acceleration measurement.

concern the main disadvantage of the model, which reflects an important sensibility to the quality of the leader acceleration measurement. In fact, during implementation we use the leader velocity measurements instead of the acceleration ones. This was possible thanks to the integrability property of the model which permits to calculate the inter-distance reference and the reference acceleration in terms of the leader speed. This will be illustrated next in the Section IV-B.1.

IV. Experimental results

In this Section, we describes some experimental results of an implemented longitudinal control. The structure of the total implemented control law is depicted in figure 2. We start this Section describing the used equipment, then we describes the implemented longitudinal controller and finally we discuss the main experimental results both for a stop-and-go scenario and for a car-following scenario.

A. Equipment description

Within the framework of the ARCOS French program and in collaboration with the LIVIC[3] Laboratory, we have

[3]LIVIC is a French laboratory about the interaction between driver, vehicle and infrastructure; see http://www.inrest.fr/ur/livic

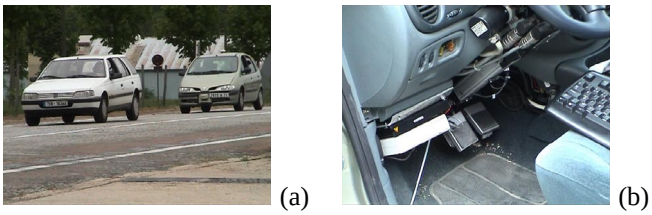

Fig. 12. (a) The LOLA car in the track and (b) its brake pedal.

obtained some preliminary experimental results. The different algorithms have been integrated on the "LOLA" test car (see figure 12).

During the test the inter-distance value is computed as the difference of the absolute position of each vehicle. The absolute position and the speed are obtained from an odometer available in each vehicle. The measures are transmitted by radio-frequency to the central computer-station located into the follower car. These values are both used for control (reference model and control feedback), and for recording in real-time. Leader and follower vehicle accelerations are obtained from their gyros (inertial sensors) with the purpose of appreciate its behavior.

B. Implemented longitudinal controller

The automotive longitudinal control is generally composed by two loops: an internal or inner control loop which compensates the nonlinear vehicle dynamics (acceleration and brake systems), and an outer control loop which is responsible for guaranteeing a good tracking of the desired reference inter-distance (given by the reference model).

The inner control loop, i.e. the throtle/brake control loop, is a non-trivial control problem. The difficulty is due to the complexity, and lack of symmetry of the throttle and brake sub-systems that control the vehicle acceleration and deceleration. In addition, the vehicle dynamics is highly non linear and behaves differently than our idealized point mass.

This important topic has been tackled elsewhere (the interested readers can be refereed to [3] and [13]). In this paper, we assume a perfect inner controller performance, yielding

$$\ddot{x}_f \simeq u, \tag{32}$$

where u stands for the outer controller output signal. Figure 13 illustrates an actuator test (i.e. the inner control loop) in the LOLA car for an arbitrary reference acceleration. Thus, we can accept the above assumption, equation (32) in the rest of the section.

In this work we are only interested in the design of an outer control loop. Here the outer controller is composed for both the reference model dynamics and an additional regulation feedback. The latter will be responsible to guarantee a compensation of non-modelled and neglected dynamics in assumption (32). Next, we describe briefly every element of the implemented longitudinal control.

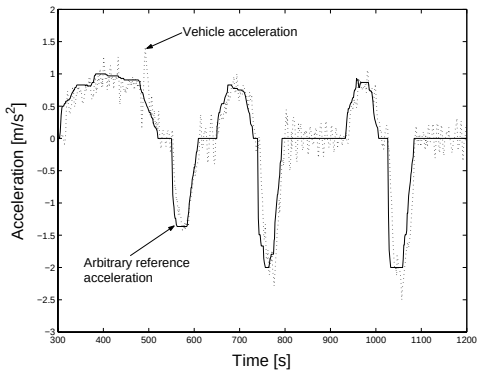

Fig. 13. An actuator test (inner control loop) in the LOLA car.

1) The reference model - A feedforward term: The reference model acts as a feedforward term into the longitudinal control law. This control action is described by the following nominal inter-distance dynamics given by equation (9). In terms of d^r we have:

$$\dot{d}^r = \frac{c}{2}(d_o - d^r)^2 + \hat{\dot{x}}_l - \beta, \tag{33}$$

where $\beta = V_{max}$. Notice that we have an input, $\hat{\dot{x}}_l$, and two outputs u^r and d^r. The output u^r is obtained from

$$u^r = c|d_o - d^r|\dot{d}^r. \tag{34}$$

The parameters c and d_o are calculated from (20) and (19) respectively. The model parameters are summarized in Table II. The initial condition $d^r(0)$ is calculated as $d^r(0) = \hat{d}(0)$, where $\hat{d}(0)$ stands for the initial inter-distance estimation or measurement.

Notice that this part of the control uses directly the solution of (9) instead of (8) itself. Thanks of this property (integrability of the model), the input required to drive the reference model will be the estimated leader velocity instead of the estimated leader acceleration. This aspect is well appreciated during the control implementation due to the fact that the leader velocity estimation is, in general, more easy to estimate, and often presents better signal-noise ratio.

2) Control feedback - A model matching: Take the inter-distance dynamics (3), i.e.

$$\ddot{d} = \ddot{x}_l - \ddot{x}_f. \tag{35}$$

Assuming that the follower vehicle acceleration (32) could be described as follow:

$$\ddot{x}_f = u + \eta_u, \tag{36}$$

where η_u stands for an inner control loop inaccuracy.

And defining $\tilde{d}_e \triangleq d^r - d$ as the tracking error signal, with d^r subject to (33) and d subject to (35). Then, the problem is to design a control feedback u that minimizes the tracking error $\tilde{d}_e$. During experiments, the chosen control structure has the following form:

$$u = u^r - H(s)\left[d^r - \hat{d}\right], \tag{37}$$

where u^r is given by (34), and $H(s)$ corresponds to a linear feedback operator.

Substituting (35) in (37) and using (4) we have:

$$\ddot{d} = \ddot{x}_l - \hat{\ddot{x}}_l + \ddot{d}^r + H(s)(\tilde{d}_e - \eta_d(t)) - \eta_u, \tag{38}$$

where $\hat{d} = d + \eta_d(t)$, and $\hat{\ddot{x}}_l = \ddot{x}_l + \eta_y(t)$. This yields the following tracking error dynamics

$$\ddot{\tilde{d}}_e + H(s)\tilde{d}_e = \eta_y(t) + H(s)\eta_d(t) + \eta_u, \tag{39}$$

with η_d, and η_y being the measurement noise associated to their respectively measures. We can re-write (39) in its equivalent Laplace representation as:

$$\tilde{d}_e = \frac{1}{s^2 + H(s)}(\eta_y + \eta_u) + \frac{H(s)}{s^2 + H(s)}\eta_d. \tag{40}$$

This means that increasing accuracy in signal $\hat{d}$, we can effectively compensate both the leader estimation uncertainties η_y and the inner control loop inaccuracy η_u for increasing the $H(s)$ gain. Hence, we could chose $H(s)$ to account for the specific frequency properties of η_d, and η_y.

Note also that the term $H(s)$ is taken here as a linear operator of the measured tracking error $(d^r - \hat{d})$. However, this feedback compensation could be obtained from more elaborated control designs, as for example H_∞/H_2 control, optimal control, state feedback, etc.

C. Results discussion

1) Case 1: A Stop-and-go scenario: The Figures 14a, 14b, 14c and 14d, correspond to the inter-distances, velocities, acceleration/deceleration, and jerks respectively during a stop-and-go scenario. Notice that we have different initial conditions (i.e. the reference inter-distance and the actual inter-distance at $t = 40s$). However the controller was charged of the attractiveness of the system states to the reference model states.

During the experimental tests we have used a Proportional-Derivative (PD) controller as the function $H(s)$. The Table III summarizes the PD-gains which give goods results (models of sensors noise was not available, so, a trial and error PD-gains adjustment was used). Due to the elevated noise in the inter-distance measurement, the controller bandwidth (dictated from the PD-gains) has been quite limited, and then, the tracking error becomes appreciable.

The reference model was adjusted using the parameters values depicted in Table II. The maximal deceleration was decreased to $7m/s^2$ in order to compensates the low bandwidth of the control feedback (i.e. smaller deceleration and jerk magnitudes require less controller bandwidth).

Notice that the jerk is so smaller and consequently better in terms of comfort. The jerk is not obtained directly from measurements, actually the jerk is calculated from derivation of acceleration measurements with suitable filtering. In fact,

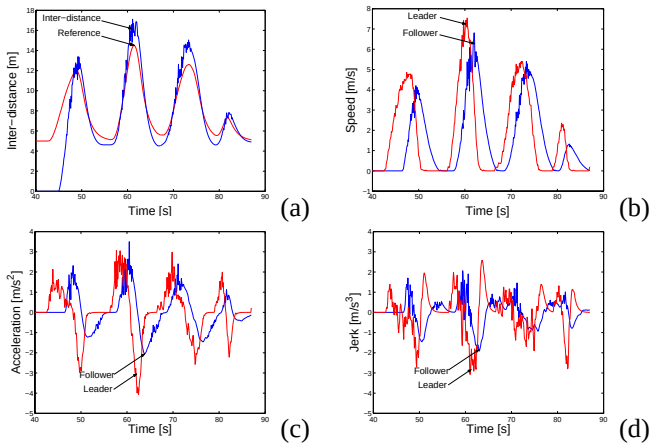

Fig. 14. Inter-distance, velocities, acceleration and jerk from experiment. A stop-and-go scenario.

TABLE II

REFERENCE MODEL PARAMETERS USED DURING EXPERIMENTS

Sample time	T_s	:	0.1 s
Maximal velocity	V_{max}	:	30 m/s
Max. braking capacity	B_{max}	:	7 m/s^2
Minimal distance	d_c	:	5 m
Max. distance	d_0	:	104 m
Parameter	c	:	0.006125

the Figure 14d is depicted in order to illustrate the magnitude of the obtained comfort.

2) Case 2: A Car-following with Hard stop scenario: The figures 15a, 15b, 15c and 15d, correspond to the inter-distances, velocities, acceleration/deceleration, and jerks respectively, during a car-following with hard stop scenario.

During car-following (i.e. between $25s$ and $57s$), the inter-distance tracking error behavior is very acceptable, with accelerations and jerks so smaller. However, during the hard stop scenario (after $57s$), the leader speed decreases abruptly with a deceleration near to $8m/s^2$. The speeds were almost $20m/s$ just before to start the braking maneuver. The follower vehicle makes use of its maximal braking capacity, exceeding the maximal braking performed by the model. This behavior is attributed to a large time delay in the inner control loop (about $300ms$ inherent to the used brake actuator/controller), which becomes appreciable during a hard stop scenario. As a consequence of this time delay, a large deceleration and an elevated positive jerk are reached. However, this jerk magnitude is raisonnable according to the scenario. In fact, this scenario is quite extreme, permitting to test the effectiveness of the proposed approach, specially the fact to avoid a collision. In addition, this positive jerk occurs near to zero speed and therefore the related uncomfort is not so perceptible in practice (see for example [7]).

V. CONCLUSION

In this paper we have presented a novel reference model-based control approach for automotive longitudinal control.

TABLE III

CONTROL FEEDBACK PARAMETERS

Proportional action gain	K_p	:	0.3
Derivative action gain	K_d	:	1.0

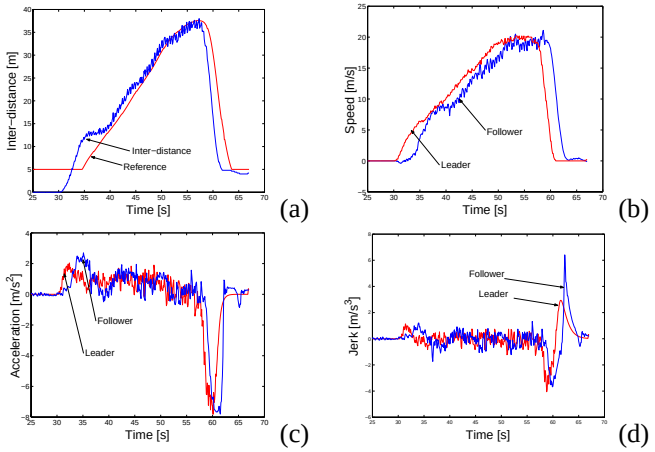

Fig. 15. Inter-distance, velocities, acceleration and jerk from experiment. A car-following scenario.

The proposed structure combines an exogen reference model with an additional control loop. The former is charged of verify some safety and comfort constraints, while the latter is charged of the model-matching between the model and the actual system, assuring a good tracking of the desired reference inter-distance.

The model has few parameters that can be also set in accord to other external factors, such as the road conditions and the traffic load. In this work, the main assumption concern the fact that the parameters model are invariant. As a future work, adaptability of the model with respect to the external information should be studied.

The proposed model is described by a nonlinear set of equations that are driven by the vehicle leader acceleration. This last aspect corresponds to the main disadvantage of the model. In fact the model requires a good estimation of the leader acceleration that could be relatively difficult to obtain directly. Nevertheless, thanks of the integrability of the model, this problem could be solved by expressing the reference inter-distance and the reference acceleration in terms of the leader speed.

Although this approach seems quite similar to some early works, for example [6], [4], and [20], where an impedance control is proposed, the distance policy presented in this paper is obtained from an exogen dynamical motion equation, instead of non-exogen stationary ones based on the classical safe distance, equation(1). This fact allows to calculated explicitly the bounds of the model solutions which are obtained through suitable integral curves. Thus, the proposed reference model does not suffer the problems discussed in Section I-A. In addition, the proposed distance policy gives

both the reference inter-distance and the necessary acceleration/deceleration, leaving an additional control loop to compensate other no modelling dynamics of the car and external perturbations. The design of the control is independent of the reference model design. Therefore, more elaborated control strategies could be used for this task.

Contrary to the other methods, the proposed control does not divise each scenario, and does not need to build different references and controllers for each one. The proposed model verify safety and comfort for all the range of speed, and in this way the proposed longitudinal control could be useful into highways and suburban areas, in particular in stop-and-go scenarios.

The string stability problem is not analyzed here. This problem together with the acceptability of this approach in commercial cars could be the object of future works.

APPENDIX I
DERIVATION OF THE MAXIMUM REFERENCE ACCELERATION AND BRAKING

Take the equation describing the dynamics of a reference vehicle, equation (14). The reference vehicle acceleration could be described in terms of $\tilde{d}$ as follow:

$$\ddot{x}_f^r = \frac{c^2}{2}\tilde{d}^3 - c(\beta - \hat{\dot{x}}_l)\tilde{d}, \tag{41}$$

where the constant β is defined in terms of the reference-model initial conditions , i.e. $\beta \triangleq \dot{x}_f^r(0) + \frac{c}{2}\tilde{d}^2(0)$. See Section III.

The maximum penetration distance, denoted as $\tilde{d}_{max} \triangleq \max_{\forall t}\{\tilde{d}(t)\}$, have been calculated from equation (12) as follow:

$$\tilde{d}_{max} \triangleq \sqrt{\frac{2\beta}{c}}, \tag{42}$$

for all $0 \leq \dot{x}_f^r(t) \leq \beta$, $\forall t$.

In addition, from equations (11) and (14) we can obtain the following boundary conditions:

$$\ddot{x}_f^r = 0, \quad \dot{x}_f^r = \beta \quad \text{at } \tilde{d} = 0 \tag{43}$$

$$\ddot{x}_f^r = 0, \quad \dot{x}_f^r = 0 \quad \text{at } \tilde{d} = \tilde{d}_{max}. \tag{44}$$

Figure 16 illustrates the reference model braking and/or acceleration for $\hat{\dot{x}}_l = 0$.

A. Maximum Braking

Taking the equations (41)-(44), and based in the figure 16, we have that

$$\min_t\{\ddot{x}_f^r(t)\} \equiv \min_{\tilde{d}}\{\ddot{x}_f^r(\tilde{d})|_{\dot{x}_l=0}\}, \tag{45}$$

i.e. the maximum value of the reference braking could be calculate from

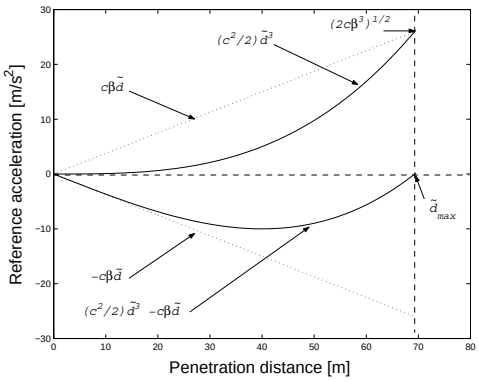

Fig. 16. The reference acceleration decomposed in two different functions, where $\max\{c(\beta - \hat{\dot{x}}_l)\tilde{d}\} = c\beta\tilde{d}$.

$$\frac{\partial \ddot{x}_f^r}{\partial \tilde{d}} = 0, \quad \text{for } \dot{x}_l = 0, \tag{46}$$

that is

$$\frac{\partial \ddot{x}_f^r}{\partial \tilde{d}} = \frac{c^2}{2}(\tilde{d}^*)^3 - c\beta\tilde{d}^* = 0. \tag{47}$$

Where the index "$*$" stands for an extremal of the function (41). Solving (47) we obtain

$$\tilde{d}^* = \sqrt{\frac{2\beta}{3c}} \tag{48}$$

which verifies $\frac{\partial^2 \ddot{x}_f^r}{\partial \tilde{d}^2}|_{\tilde{d}=\tilde{d}^*} = 3c^2\tilde{d}^* > 0$, i.e. $\tilde{d}^*$ minimizes the function (41), and the maximum braking could be calculated as

$$\min\{\ddot{x}_f^r(t)\} = -\frac{2}{3}\beta\sqrt{\frac{2c\beta}{3}}, \quad \forall t \tag{49}$$

or, in other words,

$$\ddot{x}_f^r(t) \geq -\frac{2}{3}\beta\sqrt{\frac{2c\beta}{3}}, \quad \forall t \tag{50}$$

Notice that the equation (50) determines the maximum value of the reference vehicle braking. This value depends of both the parameter c and the constant β. Remember that β is calculated from the model initial conditions.

B. Maximum Acceleration

Proceeding in the same way that in Section I-A, we can obtain a maximal bound of the reference positive acceleration. That is

$$\ddot{x}_f^r(t) \leq \frac{c^2}{2}\tilde{d}_{max}^3 = \frac{c^2}{2}\left(\frac{2\beta}{c}\right)^{\frac{3}{2}} = (2c\beta^3)^{\frac{1}{2}}, \tag{51}$$

at $\tilde{d} = \tilde{d}_{max}$ and assuming that $\hat{\dot{x}}_l$ instantaneously reaches the maximal value $\hat{\dot{x}}_l = \beta$, i.e. assuming infinite leader acceleration, and then $-c(\beta - \hat{\dot{x}}_l)\tilde{d} = 0$. Notice from the figure 16, that this bound could be so large, and then so conservative.

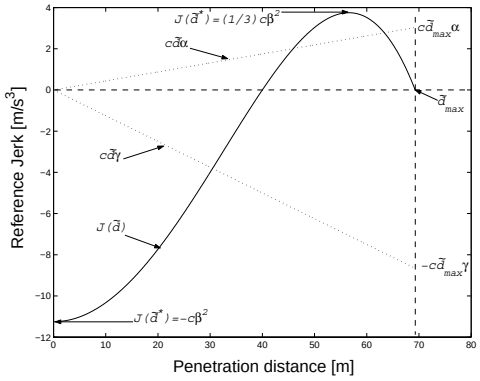

Fig. 17. The reference jerk decomposed in two different functions.

Another way to calculate the positive reference acceleration could be taking into account a bound in the estimated leader acceleration, that is, assuming that:

$$\ddot{\hat{x}}_l(t) \leq \alpha. \tag{52}$$

Using the above assumption, we will calculate $\frac{d}{dt}\ddot{x}_f^r(t) = 0$, i.e.

$$\frac{d}{dt}\ddot{x}_f^r(t) = -c(\dot{\tilde{d}}^*)^2 - c\tilde{d}^*(-c\tilde{d}^*\dot{\tilde{d}}^* - \ddot{\hat{x}}_l(t)) = 0 \tag{53}$$

Notice that into this equation it appears explicitly the leader vehicle acceleration $\ddot{\hat{x}}_l(t)$. Then, the following equation gives a condition for existence of an extremal of $\ddot{x}_f^r(t)$ as a function of $\ddot{\hat{x}}_l(t)$. So, after simplifications, we have

$$-c\tilde{d}^*\dot{\tilde{d}}^* = \ddot{\hat{x}}_l(t) - \frac{(\dot{\tilde{d}}^*)^2}{\tilde{d}^*}; \quad \forall \tilde{d}^* > 0 \tag{54}$$

Hence, substituting $\dddot{x}_f^{r*}(t) = -c\tilde{d}^*\dot{\tilde{d}}^*$ (by definition, see equation 7), in the above equation, we have

$$\dddot{x}_f^{r*}(t) = \ddot{\hat{x}}_l(t) - \frac{(\dot{\tilde{d}}^*)^2}{\tilde{d}^*} \leq \ddot{\hat{x}}_l(t); \quad \forall \tilde{d}^* > 0 \tag{55}$$

This is true for any $\dot{\tilde{d}}^*$ and any $\tilde{d}^* > 0$. Thus, from (55) and taking the assumption described by (52), the maximal reference acceleration is bounded as follow:

$$\ddot{x}_f^r(t) \leq \alpha \tag{56}$$

Notice that the maximum value of the reference vehicle acceleration depends of the maximum leader vehicle acceleration α.

APPENDIX II
DERIVATION OF THE MAXIMUM REFERENCE JERK

Take the equation (53) which describes the reference vehicle jerk. The jerk could be expressed in terms of $\tilde{d}$, as follow:

$$\dddot{x}_f^r = 2c^2\tilde{d}^2(\beta - \ddot{\hat{x}}_l) - \frac{3}{4}c^3\tilde{d}^4 - c(\beta - \ddot{\hat{x}}_l)^2 + c\tilde{d}\dddot{\hat{x}}_l \tag{57}$$

Take the right hand side of the above equation. Notice that the first term is always positive, the second and the third one are always negative, while the last one depends of the sign of the leader vehicle acceleration.

Proceeding similarly as in Appendix I, we first separate the equation (58) in two different functions, that is:

$$\dddot{x}_f^r = J(\tilde{d}) + c\tilde{d}\dddot{\hat{x}}_l \tag{58}$$

where $J(\tilde{d}) \triangleq 2c^2\tilde{d}^2(\beta - \ddot{\hat{x}}_l) - \frac{3}{4}c^3\tilde{d}^4 - c(\beta - \ddot{\hat{x}}_l)^2$.

So, a simple way to calculate the maximum values of jerk is described as follow: First we calculate the extremals of the nonlinear function $J(\tilde{d})$. Then, we calculate the maximum values (positive and/or negative) of the linear term $c\tilde{d}\dddot{\hat{x}}_l$, and finally, we add this value to the previous calculated extremals of $J(\tilde{d})$. This procedure gives a bound of the total function $\dddot{x}_f^r$.

Thus, the extremals of $J(\tilde{d})$ can be calculated from

$$\frac{\partial J(\tilde{d})}{\partial \tilde{d}} = 4c^2\tilde{d}^*(\beta - \ddot{\hat{x}}_l) - 3c^3\tilde{d}^{*3} = 0. \tag{59}$$

The above equation has two solutions:

$$\tilde{d}^* = 0 \ ; \quad \tilde{d}^* = \sqrt{\frac{4}{3}\frac{(\beta - \ddot{\hat{x}}_l)}{c}}. \tag{60}$$

Therefore, we have two extremals to be taken into account:

$$J(\tilde{d}^*)|_{\tilde{d}^*=0} = -c(\beta - \ddot{\hat{x}}_l)^2$$

$$J(\tilde{d}^*)|_{\tilde{d}^*=\sqrt{\frac{\beta-\ddot{\hat{x}}_l}{c}}} = \frac{1}{3}c(\beta - \ddot{\hat{x}}_l)^2$$

On the other hand, assuming $-\gamma \leq \ddot{\hat{x}}_l \leq \alpha$, $\forall t$, we have

$$-c\tilde{d}_{max}\gamma \leq c\tilde{d}\dddot{\hat{x}}_l \leq c\tilde{d}_{max}\alpha \tag{61}$$

Therefore, assuming $\sqrt{\frac{8\beta^5}{9c}} >> \gamma >> \alpha$, (i.e. negative jerk always greater than positive one), the maximum jerk will be bounded as follow:

$$|\dddot{x}_f^r(t)| = \max\{c\beta^2, c\tilde{d}_{max}\gamma\} \tag{62}$$

In others terms, using (42):

$$|\dddot{x}_f^r(t)| = \max\{c\beta^2, \sqrt{2c\beta}\gamma\} \tag{63}$$

The maximum value of jerk depends of the parameter c, the constant β (initial conditions) and also of the maximal acceleration/deceleration of the estimated leader vehicle γ.

ACKNOWLEDGMENT

The authors would like to express their gratitude to their colleagues Axel Von-Arnim and Cyril Royère from the LIVIC laboratory who kindly gave suggestions and discussion during algorithms integration and test. Thanks also to the ARCOS[4] French Program by its contribution and financial support.

[4]ARCOS is a French program on safety vehicle and secure roads. For details, see http://www.arcos2004.com

REFERENCES

[1] Chien C. and Ioannou P., "Automatic Vehicle-Following". *Proceeding of American Control Conference* 1992, Chicago, IL, pp.1748-1752.

[2] Yanakiev D. and Kanellakopoulos I., "Variable Time Headway for String Stability of Automated Heavy-Duty Vehicles", *Proc. of the 34th. IEEE Conference on Decision and Control*, New Orleans, LA, December 1995. pp. 4077- 4081.

[3] Persson M., Botling F., Hesslow E., Johansson R., "Stop & Go Controller for Adaptive Cruise Control", *Proceeding of the 1999 IEEE International Conference on Control Applications*, Hawaii, USA.

[4] Gerdes J.C., Rossetter E.J., Saur U., "Combining Lanekeeping and Vehicle Following with Hazard Maps". *Vehicle System Dynamics*, Vol.36, No.4-5, pp.391-411, 2001.

[5] Alvarez L. and Horowitz R., "Hybrid controller design for safe maneuvering in the PATH AHS architecture". *Proceeding of American Control Conference*, Albuquerque, New Mexico, pp. 2454-2459, June 1997.

[6] Hennessey M.P., Shankwitz C., Donath M., Sensor Based "Virtual Bumpers" for Collision Avoidance: Configuration Issues. In: *Proceeding of the SPIE*, Vol.2592, pp. 48-59, 1995.

[7] Hoberock L.L., "A Survey of Longitudinal Acceleration Comfort Studies in Ground Transportation Vehicles". *Journal of Dynamic System, Measurement; and Control*, pp. 76-84, June 1977.

[8] Hunt K.H. and Crossley F.R.E., "Coefficient of restitution Interpreted as damping in Vibroimpact", *Journal of Applied Mechanics*, pp. 440-445, June 1975.

[9] Marhefka D.W. and Orin D.E., "Simulation of Contact Using a Nonlinear Damping Model", *Proceeding of IEEE International Conference on Robotics and Automation*, pp. 1662-1668, Minneapolis, Minnesota, April 1996.

[10] Fancher P., Bareket Z., Ervin R., "Human-Centered Design of an Acc-With-Braking and Forward-Crash-Warning System". *Vehicle System Dynamics*, Vol. 36,No.2-3, pp. 203-223, 2001.

[11] Martinez J. and Canudas de Wit C., "Model reference control approach for safe longitudinal control". *American Control Conference*, Boston, USA. 2004.

[12] Brackstone M. and McDonald M., "Car-Following: a historical review", *Transportation Research* Part F 2, Pergamon, pp.181-196, 2000.

[13] Seiler P., Song B., Hedrick J.K., "Developmet of a Collision Avoidance System", *Society of Automotive Engineers (SAE)*, 98PC-417, 1998. 7p.

[14] Bengtsson J., "Adaptive Cruise Control and Driver Modeling", *Ph.D. Thesis*, Department of Automatic Control, Lund Institute of technology. Sweden, 2001. 91p.

[15] Germann St., and Isermann R., "Nonlinear distance and cruise control for passenger cars", *Proceeding of the American Control Conference*, Vol.5, pp.3081-3085, Seatle, Washington, June 1995.

[16] Goodrich M.A., and Boer E.R., "Designing Human-Centered Automation: Tradeoffs in Collision Avoidance System Design", *IEEE Transactions on Intelligent Transportation System*, Vol.1, No.1 pp.40-54, March 2000.

[17] Nouveliere L. "Commandes Robustes Appliquées au Control Assisté d'un Véhicle à Basse Vitésse". Ph.D. Thesis on Versailles-Saint Quentin en Yvelines University. France, 2002. 296p.

[18] Jones W., Keeping Cars from Crashing. IEEE Spectrum, Vol. 38, No.9, pp. 40-45, September 2001.

[19] Vahidi A. and Eskandarian A. "Research Advances in Intelligent Collision Avoidance and Adaptive Cruise Control". *IEEE Trans. on. Intelligent Transportation Systems*, Vol.4, No.3, pp. 143-153, September 2003.

[20] Gorjestani A., Shankwitz C. and Donath M. "Impedance Control for Truck Collision Avoidance". *Proceeding of the American Control Conference*, Chicago, Illinois, June 2000.

John-Jairo Martinez was born in Cali, Colombia. He received the B.S. degree in electrical engineering and the M.S. degree in automatic control from the Universidad del Valle, Colombia, in 1997 and 2000 respectively. He has joint to the Universidad Nacional de Colombia as a teacher assistant during the period 2001-2002. He received the Ph.D degree in automatic control from the Institut National Polytechnique de Grenoble INPG, France, in March 2005. Dr. Martinez has been an invited visitor in the Centre for Complex Dynamic Systems and Control of the Newcastle University, Australia 2005. And currently He has a post-doctoral position in the INPG, France. His main research interests include hybrid and nonlinear systems, applications of switching control theory and automotive control.

PLACE PHOTO HERE

Carlos Canudas-de-Wit Biography text here.